

## BROAD ABSORPTION LINE DISAPPEARANCE ON MULTI-YEAR TIMESCALES IN A LARGE QUASAR SAMPLE

N. FILIZ AK<sup>1,2,3</sup>, W. N. BRANDT<sup>1,2</sup>, P. B. HALL<sup>4</sup>, D. P. SCHNEIDER<sup>1,2</sup>, S. F. ANDERSON<sup>5</sup>, R. R. GIBSON<sup>5</sup>, B. F. LUNDGREN<sup>6</sup>, A. D. MYERS<sup>7</sup>, P. PETITJEAN<sup>8</sup>, NICHOLAS P. ROSS<sup>9</sup>, YUE SHEN<sup>10</sup>, D. G. YORK<sup>11</sup>, AND D. BIZYAEV<sup>12</sup>, J. BRINKMANN<sup>12</sup>, E. MALANUSHENKO<sup>12</sup>, D. J. ORAVETZ<sup>12</sup>, K. PAN<sup>12</sup>, A. E. SIMMONS<sup>12</sup>, B. A. WEAVER<sup>13</sup>

*Draft version October 29, 2018*

### ABSTRACT

We present 21 examples of C IV Broad Absorption Line (BAL) trough disappearance in 19 quasars selected from systematic multi-epoch observations of 582 bright BAL quasars ( $1.9 < z < 4.5$ ) by the Sloan Digital Sky Survey-I/II (SDSS-I/II) and SDSS-III. The observations span 1.1–3.9 yr rest-frame timescales, longer than have been sampled in many previous BAL variability studies. On these timescales,  $\approx 2.3\%$  of C IV BAL troughs disappear and  $\approx 3.3\%$  of BAL quasars show a disappearing trough. These observed frequencies suggest that many C IV BAL absorbers spend on average at most a century along our line of sight to their quasar. Ten of the 19 BAL quasars showing C IV BAL disappearance have apparently transformed from BAL to non-BAL quasars; these are the first reported examples of such transformations. The BAL troughs that disappear tend to be those with small-to-moderate equivalent widths, relatively shallow depths, and high outflow velocities. Other non-disappearing C IV BALs in those nine objects having multiple troughs tend to weaken when one of them disappears, indicating a connection between the disappearing and non-disappearing troughs, even for velocity separations as large as  $10000\text{--}15000 \text{ km s}^{-1}$ . We discuss possible origins of this connection including disk-wind rotation and changes in shielding gas.

*Subject headings:* galaxies: quasars: absorption lines

### 1. INTRODUCTION

Intrinsic absorption lines in quasar spectra are often produced by outflowing winds along the line of sight that are launched from the accretion disk or other structures around the central supermassive black hole (SMBH; e.g., Murray et al. 1995; Proga et al. 2000). Such absorption lines, shaped by the geometry and kinematic structure of the outflows, appear in quasar spectra as broad absorption lines (BALs;  $\Delta v \geq 2000 \text{ km s}^{-1}$ ), mini-BALs ( $2000 \geq \Delta v \geq 500 \text{ km s}^{-1}$ ), or intrinsic narrow absorption lines (NALs;  $\Delta v \leq 500 \text{ km s}^{-1}$ ); e.g., see Hamann et al. (2008) and Ganguly & Brotherton (2008). Traditionally defined BAL troughs are observed in  $\approx 15\%$  of quasars; these troughs are sufficiently strong that the depths of the features

lie at least 10% under the continuum in the, e.g., Si IV  $\lambda 1400$ , C IV  $\lambda 1549$ , Al III  $\lambda 1857$ , or Mg II  $\lambda 2799$  transitions with blueshifted velocities up to  $\approx 0.1c$  (e.g., Weymann et al. 1991; Gibson et al. 2009, hereafter G09; Allen et al. 2011; and references therein). Quasars that present BAL troughs in their spectra are often classified into three subtypes depending on the presence of absorption lines in specified transitions: (1) High-ionization BAL quasars show absorption lines in high-ionization transitions including Si IV, and C IV. (2) Low-ionization BAL quasars possess Mg II and/or Al III absorption lines, in addition to the high-ionization transitions. (3) Iron low-ionization BAL quasars show additional absorption from excited states of Fe II and Fe III (e.g., Hall et al. 2002, and references therein).

The winds revealed by intrinsic quasar absorption lines are of importance for two main reasons. First, the observed frequency of quasar absorption lines indicates that these winds are a significant component of the nuclear environment. Indeed, disk accretion onto the SMBH may require significant mass ejection for expulsion of angular momentum from the system (e.g., Blandford & Payne 1982; Crenshaw et al. 2003). Second, quasar winds may be agents of feedback into massive galaxies, regulating star formation and further SMBH accretion via the removal of cold gas (e.g., Springel et al. 2005; King 2010).

BAL troughs, the strongest observed signatures of quasar winds, often vary in equivalent width (EW) and/or shape over rest-frame timescales of months to years (e.g., Barlow 1993; Lundgren et al. 2007; Gibson et al. 2008, 2010; Capellupo et al. 2011, 2012). Recent statistical studies of BAL variability have shown that the fractional EW change increases with rest-frame timescale over the range 0.05–5 yr. Such variations could, in principle, be driven by changes in covering factor, velocity structure, or ionization level. Of these possibilities, the generally favored driver for most BAL variations is changes in the covering factor of outflow stream lines that partially block the continuum emis-

Electronic address: nfilizak@astro.psu.edu

<sup>1</sup> Department of Astronomy & Astrophysics, Pennsylvania State University, University Park, PA, 16802, USA

<sup>2</sup> Institute for Gravitation and the Cosmos, Pennsylvania State University, University Park, PA 16802, USA

<sup>3</sup> Faculty of Sciences, Department of Astronomy and Space Sciences, Erciyes University, 38039 Kayseri, Turkey

<sup>4</sup> Department of Physics and Astronomy, York University, 4700 Keele St., Toronto, Ontario, M3J 1P3, Canada

<sup>5</sup> Astronomy Department, University of Washington, Seattle, WA 98195, USA

<sup>6</sup> Department of Physics, Yale University, New Haven, CT 06511, USA

<sup>7</sup> Department of Physics and Astronomy, University of Wyoming, Laramie, WY 82071, USA

<sup>8</sup> Universite Paris 6, Institut d'Astrophysique de Paris, 75014, Paris, France

<sup>9</sup> Lawrence Berkeley National Laboratory, 1 Cyclotron Road, Berkeley, CA 92420, USA

<sup>10</sup> Harvard-Smithsonian Center for Astrophysics, 60 Garden St., MS-51, Cambridge, MA 02138, USA

<sup>11</sup> Department of Astronomy & Astrophysics, and Enrico Fermi Institute, The University of Chicago, 5640 S. Ellis Ave., Chicago, IL 60637, USA

<sup>12</sup> Apache Point Observatory, P.O. Box 59, Sunspot, NM 88349-0059, USA

<sup>13</sup> Center for Cosmology and Particle Physics, New York University, New York, NY 10003 USA

sion (e.g., Hamann 1998; Arav et al. 1999). These covering-factor changes could ultimately be caused by rotation of a non-axisymmetric outflow that is loosely anchored to the accretion disk, or they could arise from large-scale changes in wind structure (e.g., Proga et al. 2000). Changes in ionization level are generally disfavored as a primary driver, since BAL troughs are often highly saturated and thus should be only weakly responsive to ionization-level changes. Furthermore, BAL trough variations generally do not appear to be correlated with variations of the observable continuum (typically longward of  $\text{Ly}\alpha$  (e.g., Gibson et al. 2008), although the observable continuum is not the ionizing continuum for the BAL gas (i.e., it is possible that the two may vary differently).

Strong variations in BAL EWs observed over multi-year timescales in the rest frame suggest that BAL disappearance and BAL emergence may be significant effects on such timescales (e.g., Gibson et al. 2008; Hall et al. 2011). However, largely owing to practical difficulties in observing large samples of BAL quasars on multi-year timescales (often corresponding to 10–20 yr in the observed frame), only a small number of BAL disappearance (Junkkarinen et al. 2001; Lundgren et al. 2007; Hall et al. 2011; Vivek et al. 2012) and emergence (Ma 2002; Lundgren et al. 2007; Hamann et al. 2008; Leighly et al. 2009; Krongold et al. 2010; Capellupo et al. 2012; Vivek et al. 2012) events have been discovered. Specifically, considering the BAL disappearance phenomenon of most relevance to this paper, we are only aware of four reported cases. In the first, a Mg II BAL in the spectrum of the binary quasar LBQS 0103–2753 essentially disappeared over  $\leq 6.0$  rest-frame years, converting this object from a low-ionization BAL quasar to a high-ionization BAL quasar (Junkkarinen et al. 2001). In the second, the highest velocity C IV trough in the spectrum of J075010.17+304032.3 nearly disappeared in  $\leq 0.3$  rest-frame years, which is the only known example of C IV disappearance (Lundgren et al. 2007). In the third, the Fe II troughs in the spectrum of FBQS J1408+3054 disappeared over  $\leq 5.1$  rest-frame years, converting this object from an iron low-ionization BAL quasar to a low-ionization BAL quasar (Hall et al. 2011). In the fourth, a Mg II BAL trough in the spectrum of SDSS J133356.02+001229.1 disappeared in  $\leq 3.7$  rest-frame years and another Mg II BAL trough — that emerged at higher velocity — nearly disappeared in  $\leq 5.7$  rest-frame years (Vivek et al. 2012). These disappearance examples did not involve transformations from BAL quasars to non-BAL quasar status because troughs from other ions, or additional C IV troughs, remained.

We have compiled a sample of 19 quasars with disappearing BAL troughs from a well-defined, large sample of BAL quasars whose spectra were observed over 1.1–3.9 yr in the rest frame. We aim to define the basic statistical characteristics of the BAL disappearance phenomenon. In this study, we will discuss the disappearance of BAL troughs as well as the transformation of BAL quasars to non-BAL quasars. These two phenomena can be distinct given that some BAL quasars have multiple troughs. A quasar that possesses more than one BAL trough could have only one of them disappear without transforming to a non-BAL quasar. We only consider BAL quasars without any remaining BAL troughs at a later epoch (in any transition) to have transformed from a BAL quasar to a non-BAL quasar. The observations and the selection of the main sample used in this study are discussed in §2. Identification of disappearing BAL troughs is explained in §3. Statistical results and comparisons are presented in §4. A summary

of the main results and some future prospects are given in §5.

Throughout this work we use a cosmology in which  $H_0 = 70 \text{ km s}^{-1} \text{ Mpc}^{-1}$ ,  $\Omega_M = 0.3$ , and  $\Omega_\Lambda = 0.7$ . All timescales are in the rest frame unless otherwise mentioned.

## 2. OBSERVATIONS AND SAMPLE SELECTION

### 2.1. Observations

The Baryon Oscillation Spectroscopic Survey (BOSS), part of the Sloan Digital Sky Survey-III (SDSS-III; Eisenstein et al. 2011), is a five-year program (2009–2014) that is using the 2.5-m SDSS telescope (Gunn et al. 2006) at Apache Point Observatory to obtain spectra for  $\approx 1.5$  million luminous galaxies as well as  $\approx 160,000$  quasars at  $z > 2.2$  (Anderson et al. 2012; Ross et al. 2012). These targets are selected from  $\approx 10,000 \text{ deg}^2$  of sky at high Galactic latitude. While the primary goal of BOSS is to obtain precision measurements of the cosmic distance scale using baryon acoustic oscillations, the resulting spectra (covering 3600–10000 Å at a resolution of 1300–3000; see Eisenstein et al. 2011) are valuable for a wide range of investigations, including studies of quasar physics.

In addition to the main BOSS galaxy and quasar surveys, a number of smaller ancillary BOSS projects are being executed. One of these ancillary projects, relevant to this paper, focuses on studying BAL variability on multi-year timescales in the rest frame. The main goal of this project is to move from small-sample and single-object studies of multi-year BAL variability to setting large-sample statistical constraints that can ultimately be compared with models of quasar winds. The basic approach is to obtain BOSS spectroscopy of BAL quasars already observed from 2000–2008 by SDSS-I/II. Most of the targets for this project are drawn from the G09 catalog of 5039 BAL quasars in the SDSS Data Release (DR) 5 quasar catalog (Schneider et al. 2007). Specifically, we have selected the 2005 BAL quasars from this catalog that are optically bright ( $i < 19.3$ ); have high signal-to-noise ratio SDSS-I/II spectra ( $\text{SN}_{1700} > 6$  as defined by G09, when  $\text{SN}_{1700}$  measurements are available); have full spectral coverage of their C IV, Si IV, Mg II, or Al III BAL regions (implemented via the redshift cuts described in §4 of G09); and have moderately strong to strong BAL troughs (balnicity indices of  $\text{BI}_0 > 100 \text{ km s}^{-1}$  as defined by G09). This uniformly defined sample is  $\approx 100$  times larger than current data sets that have been used to study BAL variability on multi-year timescales in the rest-frame (e.g., Gibson et al. 2008, 2010; Capellupo et al. 2011, 2012). We are also targeting 102 additional BAL quasars selected to include unusual BAL quasars (e.g., Hall et al. 2002); objects with multiple SDSS-I/II observations; and objects with historical coverage by the Large Bright Quasar Survey (e.g., Hewett et al. 1995) or the First Bright Quasar Survey (e.g., White et al. 2000).

Observations for our ancillary project began at the same time as the primary BOSS observations, and in this paper we will utilize spectra taken after the end of hardware commissioning (MJD 55176; see Ross et al. 2012) until MJD 55811 (i.e., 2009 December 11 until 2011 September 7). Within this date range, 692 of our 2005 primary BAL quasars were targeted, and observations for this program will continue throughout the BOSS project.

### 2.2. Sample Selection

For the purpose of the BAL disappearance studies in this paper, we have selected a subset of the 2005 targeted BAL

quasars with both SDSS-I/II and BOSS observations that satisfy our selection criteria given in §2.1 — all 102 unusual and other BAL quasars are excluded. We will focus on C IV BALs, as this is the most commonly studied strong BAL transition and has limited blending and confusion with other nearby transitions. Following §4 of G09, we therefore consider only those BAL quasars in the redshift range  $z = 1.68\text{--}4.93$  where the SDSS-I/II spectra provide full coverage of the C IV region.

As in past work (e.g., Lundgren et al. 2007), we only consider C IV BAL troughs that are significantly detached from the C IV emission line; this selection minimizes the chance of confusion between BAL variability and emission-line variability. To implement this requirement formally, we consider only those C IV BAL trough regions lying in the velocity range of  $-30000 \leq v_{\max} < -3000 \text{ km s}^{-1}$  ( $v_{\max}$  is the maximum observed velocity for the BAL trough region and is defined fully in §3.2). We show in §4.3 that this requirement should not significantly bias our statistical results. The  $v_{\max} \geq -30000 \text{ km s}^{-1}$  requirement minimizes confusion between C IV BALs and the Si IV emission line.

The selections above result in 582 BAL quasars which we define as our “main sample”. By construction, all of these quasars have at least one SDSS-I/II spectrum and one BOSS spectrum. A significant minority have additional SDSS-I/II or BOSS spectra. In total, we have 1396 spectra for the 582 main-sample BAL quasars. The rest-frame time intervals between spectral observations range from 0.26 days to 3.86 yr, although in this paper our emphasis will be on  $> 1$  yr timescales.

Figure 1 shows the average total EW versus the maximum sampled rest-frame timescale,  $\Delta t_{\max}$ . The EW values of all C IV BAL troughs in a given spectrum are summed and averaged over two epochs (the first SDSS and last BOSS spectrum). The maximum timescales for our sample range between 1.10 and 3.88 yr, with a mean of 2.52 yr and a median of 2.50 yr. For comparison, we have also plotted several other samples of BAL quasars whose BAL variability properties have been previously investigated (Barlow 1993; Lundgren et al. 2007; Gibson et al. 2008; Capellupo et al. 2011). Note the relatively large size of our sample compared to past work as well as the fairly long timescales being probed.

We have cross correlated our 582 main-sample BAL quasars with the Shen et al. (2011) catalog to check for radio emission detected in Very Large Array (VLA) Faint Images of the Radio Sky at Twenty-Centimeters (FIRST; Becker et al. 1995) observations. Shen et al. (2011) list the radio-loudness parameter defined as  $R = f_{6\text{cm}}/f_{2500}$ , where  $f_{6\text{cm}}$  is the radio flux density at rest-frame 6 cm and  $f_{2500}$  is the optical flux density at rest-frame 2500 Å. We also have examined the NRAO VLA Sky Survey (NVSS; Condon et al. 1998) for three quasars that are not located in the FIRST footprint. Radio emission is detected from 55 of the main-sample quasars; seven of them are radio loud with  $R \geq 100$ .

### 3. IDENTIFICATION OF DISAPPEARING BALs

#### 3.1. Continuum Fit and Normalization

To study variations in BAL characteristics, we investigate multi-epoch spectra that are normalized by an estimated continuum model. To determine proper continuum levels, we first corrected the main-sample spectra for Galactic extinction using a Milky Way extinction model (Cardelli et al. 1989) for  $R_V = 3.1$ . The  $A_V$  values were taken from the Schlegel et al. (1998). We then translated observed wavelengths to the rest frame using redshifts from Hewett & Wild (2010).

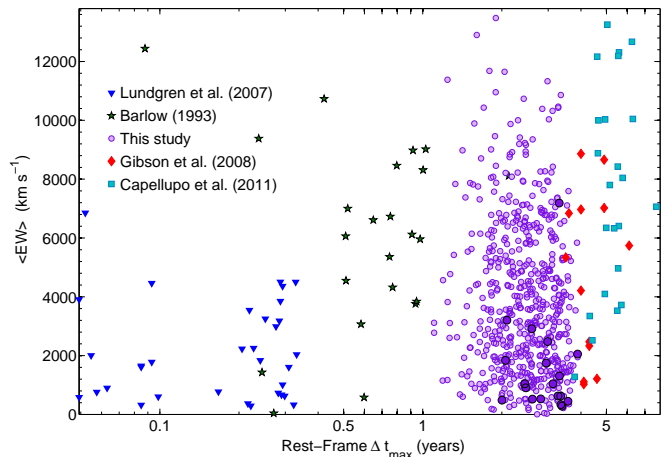


FIG. 1.— Comparison of the total rest-frame EWs (summed over all BAL troughs and averaged over two epochs) of the C IV BALs for the sources in Barlow (1993; green stars), Lundgren et al. (2007; blue triangles), Gibson et al. (2008; red diamonds), Capellupo et al. (2011; cyan squares), and our study of the 582 BAL quasars in the main sample (purple circles). The  $x$ -axis shows the maximum sampled timescale in the rest frame. Dark purple circles denote the quasars with disappearing troughs. The EW is shown in units of  $\text{km s}^{-1}$ ; 1 is about  $200 \text{ km s}^{-1}$  in the C IV region.

The data-reduction pipelines for SDSS I/II (DR7) and BOSS (v5\_4\_45)<sup>14</sup> remove night-sky lines from the data, but occasionally there are significant residuals near prominent night-sky lines. The data-processing algorithm flags the afflicted pixels in pixel-mask columns. We examine the “BRIGHTSKY” mask column and remove the flagged pixels from each spectrum.

As in G09, we select the following six relatively line-free (RLF) windows, if they have spectral coverage, to fit a continuum model to each spectrum: 1250–1350 Å, 1700–1800 Å, 1950–2200 Å, 2650–2710 Å, 2950–3700 Å, and 3950–4050 Å. We select these RLF windows to be free from strong emission and absorption in general and to represent the underlying continuum both blueward and redward of the C IV and Si IV BAL regions; the use of the RLF windows spanning a fairly broad range of wavelengths provides useful leverage for constraining the continuum shape. We avoid the use of any window at shorter wavelengths due to heavily absorbed regions, such as H I absorption in the Ly $\alpha$  forest.

Previous studies of BAL variability have used a variety of models to define the underlying continuum, such as power-law fits (e.g., Barlow 1993; Capellupo et al. 2011, 2012), reddened power-law fits (e.g., Gibson et al. 2008, 2009), and polynomial fits (e.g., Lundgren et al. 2007). As in G09, we prefer to use a reddened power-law that reconstructs the underlying continuum well at all covered wavelengths with a small number (three) of parameters. Hopkins et al. (2004) show that the intrinsic dust reddening in quasar spectra is dominated by Small-Magellanic-Cloud-like (SMC-like) reddening. We reconstruct the continuum with a power-law model that is intrinsically reddened using the SMC-like reddening model from Pei (1992). The three continuum-model parameters are thus the power-law normalization, the power-law spectral index, and the intrinsic-absorption coefficient.

The continuum-model parameters for each spectrum are obtained from a non-linear least-squares fit with an iterative “sigma-clipping” algorithm. The sigma-clipping filtering iteratively excludes the data points that deviate by more

<sup>14</sup> The BOSS pipeline is described in Aihara et al. (2011).

than  $3\sigma$  from the previous fit. Absorption or emission features (e.g., intervening absorption lines) that are occasionally present in the RLF windows are thereby filtered. Typically 1–8% of the RLF-window spectral pixels are excluded in a given spectrum. We calculate the continuum-model parameters with 68.3% confidence bounds (given that the average line-flux sensitivity in SDSS spectra matches the  $1\sigma$  noise; Bolton et al. 2004). We calculate the confidence bounds using numerical  $\Delta\chi^2$  confidence region estimation for three parameters of interest; see, e.g., §15.6.5 of Press et al. (2007). We propagate the derived continuum uncertainties through to continuum-normalized flux densities and EW measurements (see §3.2 and Table 2).

We do not assign physical meaning to the resulting continuum-model parameters, because (1) degeneracy in model parameters allows multiple sets of parameters to produce nearly the same continuum, and (2) flux levels in blue regions (3500–5500 Å in the observed frame) of BOSS spectra are not yet absolutely or relatively calibrated to better than  $\pm 10\%$  overall, with greater uncertainties at shorter wavelengths owing to remaining instrumental effects (e.g., Margala & Kirkby 2011). For further discussion of difficulties in the physical interpretation of continuum-model parameters, see §2.1 of Gibson et al. (2008).

Figure 2 shows the best continuum-model fits for some examples of BOSS spectra. The RLF windows for each spectrum have miscellaneous line-like features that are iteratively excluded by our sigma-clipping filtering. Visual inspection shows that our continuum-reconstruction algorithm produces appropriate continuum levels. Comparison of local continua blueward and redward of C IV BAL troughs (not in the RLF windows) shows good agreement between the data and the fitted continuum. Furthermore, there is good agreement between two epochs that are fitted independently. The reddened power-law model includes extinction that changes only slowly with wavelength and cannot produce false BALs given these local continuum constraints.

In addition to the statistical errors that we have quantified above, we also considered possible systematic errors in the continuum fitting. For example, we considered the systematic errors arising from our sigma-clipping filtering technique. As a test of the robustness of this approach, we repeated the filtering for  $2\sigma$  and  $4\sigma$  clipping and obtained essentially the same continuum fits as with  $3\sigma$  clipping. We further estimated systematic errors in continuum models with one-sided sigma-clipping filtering. Sigma clipping of only positive deviations and of only negative deviations give lower and upper bounds on the continuum, respectively. We found that the estimated systematic errors with this particular method are less than the statistical errors. Another possible systematic error could arise when the spectral region blueward of the Si IV BAL region lies near the edge of the observed spectrum where there is significant noise. However, a visual comparison of the continuum-fitting results for such objects does not show any significant difference from the others.

### 3.2. Measurements of BAL Properties

As is a common practice for BAL studies (e.g., Lundgren et al. 2007; Gibson et al. 2008, 2009), we smoothed each spectrum with a Savitzky-Golay (SG; Savitzky & Golay 1964) algorithm before investigating the BAL troughs. The SG parameters were selected to perform local linear regression on three consecutive data points that preserve the trends of slow variations and smooth the fluctuations originating

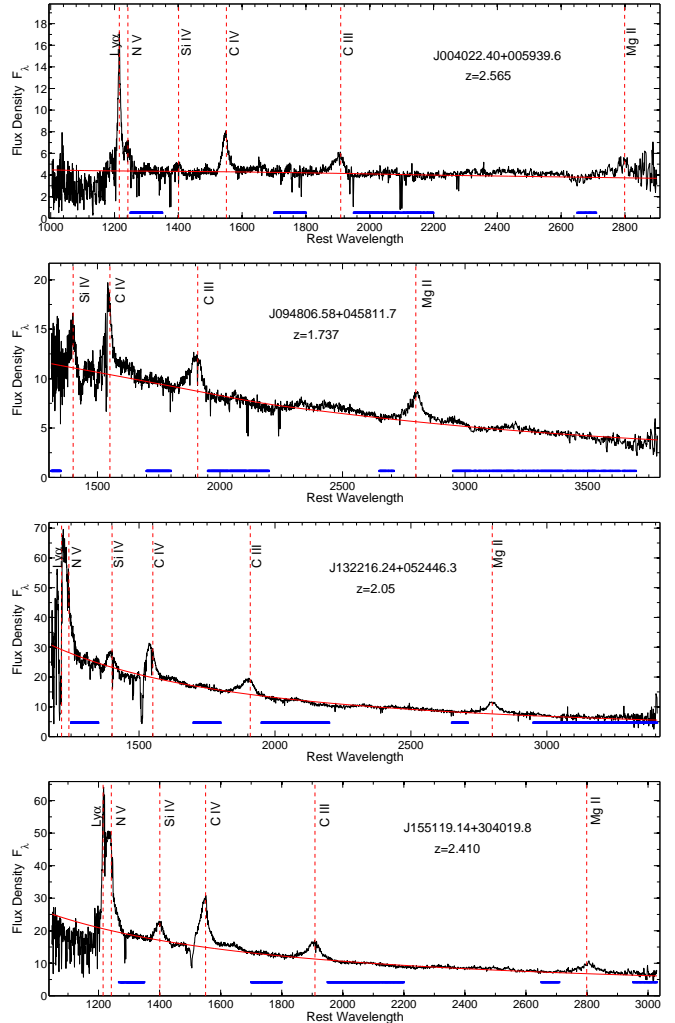


FIG. 2.— The best-fit continuum models for four example BOSS spectra of quasars with disappearing BAL troughs. The observed flux density (in units of  $10^{-17}$  erg  $\text{cm}^{-2}$   $\text{s}^{-1}$ ) and the rest-frame wavelength (in Å) of each object (black) is fitted with the continuum model (solid red) in the plotted RLF windows (blue horizontal lines). Discrete spectral features within the RLF windows were removed via the iterative continuum fitting process.

from noise. We used the smoothed spectra only to facilitate C IV BAL detection.

We searched each smoothed spectrum for absorption troughs at a level of  $\geq 10\%$  under the continuum as given in the traditional definition of BAL and mini-BAL troughs. Velocities corresponding to the shortest and the longest wavelengths for a given trough,  $v_{\text{max}}$  and  $v_{\text{min}}$  respectively, determine each trough’s width. We sorted the features into mini-BAL troughs (500–2000  $\text{km s}^{-1}$  wide) and BAL troughs ( $\geq 2000$   $\text{km s}^{-1}$  wide); see §1 for further discussion.

We detected a total of 925 distinct C IV BAL troughs in observations of 582 main-sample quasars. As described in d’2.2, we consider only troughs lying in the velocity range of  $-30000 \leq v_{\text{max}} < -3000$   $\text{km s}^{-1}$  to minimize confusion between BAL variability and emission-line variability. For a small fraction of the distinct C IV BAL troughs (15%), the trough region extends beyond the given velocity limits, mainly at the low velocity boundary. For such BAL troughs we assign the relevant cut-off velocity as the boundary of the BAL trough, and we consider the portion of the trough that lies within the given limits for further calculations. A visual comparison of the detected BAL troughs and the positions of

these troughs with those in G09 shows good general agreement.

We calculate the C IV balnicity index (BI') of each spectrum. We use a similar expression to the traditional BI definition given by Weymann et al. (1991). Our expression is

$$\text{BI}' \equiv \int_{-3000}^{-30000} \left(1 - \frac{f(v)}{0.9}\right) C dv \quad (1)$$

In this definition, BI' is expressed in units of  $\text{km s}^{-1}$  where  $f(v)$  is normalized flux density as a function of velocity, and  $C$  is a constant which is equal to 1.0 only where a trough is wider than  $2000 \text{ km s}^{-1}$ , and is 0.0 otherwise. The only difference from the traditional balnicity definition is the limiting velocities of the C IV BAL region (i.e., from  $-3000$  to  $-30000 \text{ km s}^{-1}$  instead of from  $-3000$  to  $-25000 \text{ km s}^{-1}$ ).<sup>15</sup>

We calculate the rest-frame equivalent width (EW) for each BAL trough in units of both  $\text{\AA}$  and  $\text{km s}^{-1}$ ; note that  $1 \text{ \AA}$  corresponds to  $\approx 200 \text{ km s}^{-1}$  in the C IV absorption region in the rest frame. EW and EW uncertainties are calculated from unsmoothed data using Equations 1 and 2 of Kaspi et al. (2002). In addition, following Gallagher et al. (2006), we define the  $f_{\text{deep}}^{25}$  parameter to represent the fraction of data points that lie at least 25% under the continuum level in each BAL trough.

As discussed in Gibson et al. (2008), BI' and EW measurements alone are not satisfactory for variability studies. For the purpose of better understanding spectral variations, we compared observations of a given quasar at two different epochs that were obtained with a time interval  $\Delta t$ . We define  $\Delta t$  as the rest-frame interval between the last observation showing a BAL trough (at time  $t_1$ ) and the first observation where the trough has disappeared (at time  $t_2$ ). Note that  $\Delta t$  can be different from  $\Delta t_{\text{max}}$  in §2.2 for the quasars that are observed in more than two epochs;  $\Delta t$  represents an upper limit for the disappearance time of a BAL trough with the EW value seen in the last epoch in which the trough was present. For our sample, the range of  $\Delta t$  is 1.10–3.88 yr with a mean of 2.47 yr and a median of 2.45 yr.

The BOSS spectra are provided at the same observed wavelengths as the SDSS spectra (except for the additional BOSS wavelength coverage), therefore we can compare spectra at identical wavelengths. Proper comparison requires consideration of differences in signal-to-noise ratio (S/N) incorporating standard deviations ( $\sigma$ ). Therefore, each (unsmoothed) pixel in the spectra, observed at  $t_1$  and  $t_2$ , is compared using the following calculation of the quantity  $N_\sigma$ :

$$N_\sigma(\lambda) = \frac{f_2 - f_1}{\sqrt{\sigma_2^2 + \sigma_1^2}} \quad (2)$$

where  $f_1$  and  $f_2$  are the normalized flux densities and  $\sigma_1$  and  $\sigma_2$  are the flux density standard deviations at wavelength  $\lambda$ . Both  $\sigma_1$  and  $\sigma_2$  include uncertainties from the continuum model (see §3.1), in addition to the uncertainties from the observations. To summarize  $N_\sigma$  is a measurement of the deviation between two observations for each pixel in units of  $\sigma$  (see Figure 3).

### 3.3. Selection of Disappearing BALs

BAL troughs are often complex and can be difficult to quantify with simple and standard rules. Nevertheless, we define

<sup>15</sup> Negative signs indicate that the BAL trough is blueshifted with respect to the systemic velocity.

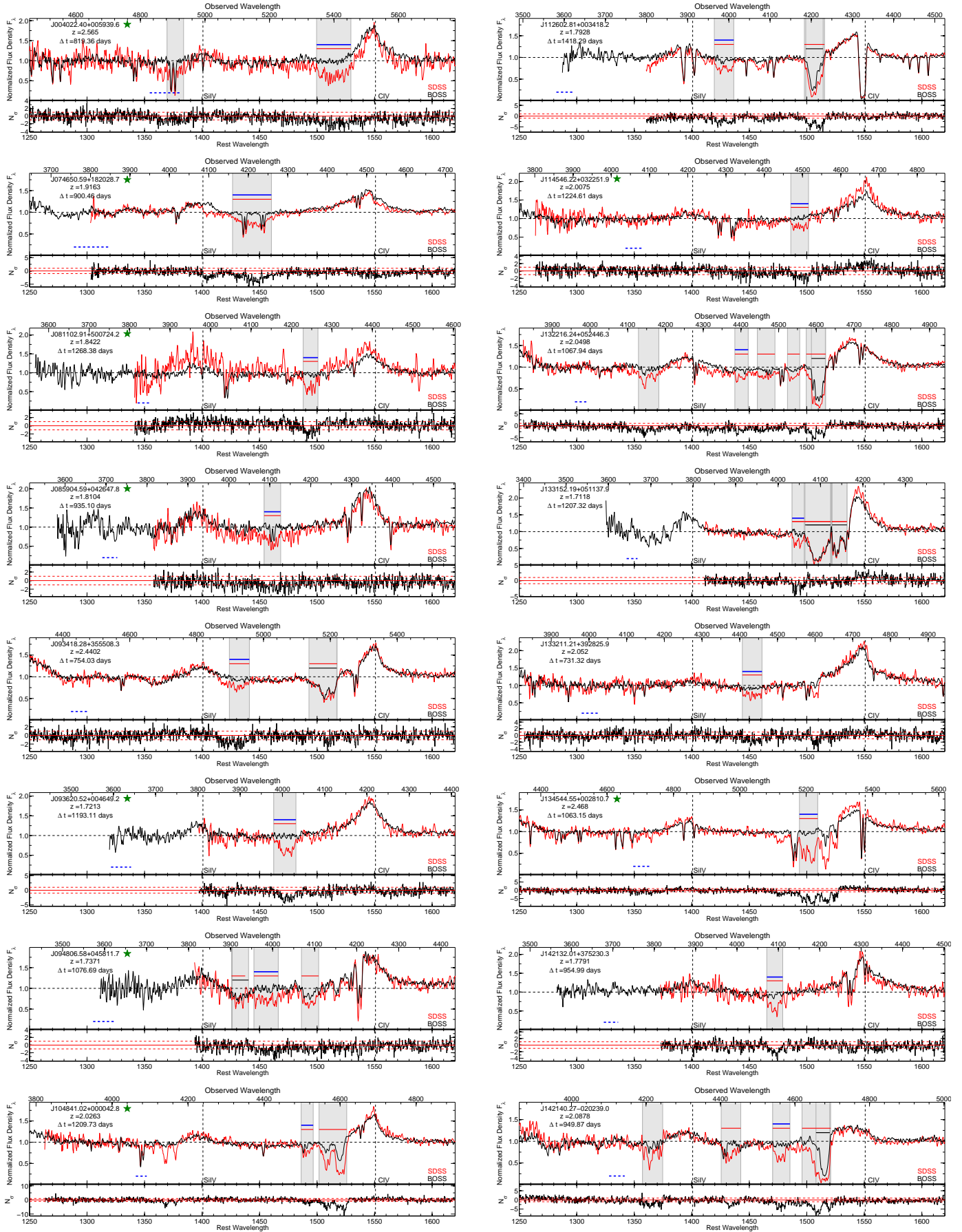
objective criteria to search all 582 main-sample BAL quasars for disappearing C IV BAL troughs. These criteria were based on the comparison between two normalized spectra,  $S_1$  and  $S_2$ , observed at epochs  $t_1$  and  $t_2$ . The utilized criteria were the following:

- The spectral region in  $S_2$  corresponding to the trough seen in  $S_1$  (lying between  $v_{\text{min}}$  and  $v_{\text{max}}$  as defined in §3.2, and corresponding to the gray shaded regions in Figure 3) should be free from any BALs or mini-BALs. However, we do allow the trough region in  $S_2$  to contain residual NALs. Our upper limit for any remaining C IV absorption in  $S_2$  will be discussed below.
- A two-sample  $\chi^2$  test (see §4.4 of Bevington & Robinson 2003) comparing the data points in the trough region between  $S_1$  and  $S_2$  gives a probability of  $P_{\chi^2} < 10^{-8}$  of there being no change. This criterion establishes that there has been a highly significant change in the trough region between  $S_1$  and  $S_2$ ; variations with less-significant values of  $P_{\chi^2}$  may be real in some cases but can be arguable allowing for both statistical and systematic errors (see §3.1), as well as the general complexity of BAL troughs. The chosen probability threshold has been selected based upon visual inspection.

Following the stated criteria, we identify 21 examples of disappearing C IV BAL troughs in 19 distinct quasars; these 19 quasars have  $\Delta t$  values of 2.0–3.3 yr. Figure 3 compares normalized SDSS and BOSS spectra in the C IV and Si IV regions for quasars with disappearing BAL troughs.  $N_\sigma$  values are also plotted for each wavelength bin.

We have defined BAL disappearance following the formal definitions of BALs and mini-BALs given in §3.2. However, in the BOSS spectra of some objects there is weak residual absorption that fails our formal definition (see §3.2 and especially Equation 1) for being a BAL or mini-BAL. We define 11 of the 21 examples of disappearing C IV BAL troughs as a “pristine” sample that has no significant remaining absorption (NAL regions excluded). These pristine sample objects are noted with stars in Figure 3. Table 1 lists all observation epochs for the quasars with disappearing BAL troughs in addition to redshifts from Hewett & Wild (2010), SDSS  $i$ -band magnitudes from Schneider et al. (2007), and absolute  $i$ -band magnitudes from Shen et al. (2011). The listed Plate-MJD-Fiber numbers are unique for each spectrum, and MJD  $\geq 55176$  indicates BOSS spectra. Table 2 lists the parameters of disappearing BAL troughs measured in  $S_1$  including observation epoch MJD, EW,  $v_{\text{max}}$ ,  $v_{\text{min}}$ ,  $f_{\text{deep}}^{25}$ , the rest-frame time interval between  $S_1$  and  $S_2$ , and  $\log(P_{\chi^2})$ .

To assess possible residual absorption remaining in the trough region of  $S_2$ , we set upper limits on EW using a  $\chi^2$  fitting approach. We assume that the absorption remaining in  $S_2$  has the same profile as that found in  $S_1$ , scaled by a constant multiplicative factor,  $\epsilon$ , lying between 0 and 1. We first find the value of  $\epsilon$  providing the best fit to the trough region in  $S_2$  (spectral regions containing NALs as described in §3.4 are excised in this analysis). We then set a 90% confidence upper limit on  $\epsilon$  by incrementing it until  $\chi^2$  increases by 2.71 from the best-fit value (see, e.g., §15.6.5 of Press et al. 2007), and we use the scaled profile with this upper limit on  $\epsilon$  to compute an upper limit on EW. Our EW limits are typically  $< 1.3 \text{ \AA}$  with a median upper limit of  $0.8 \text{ \AA}$ . We note that



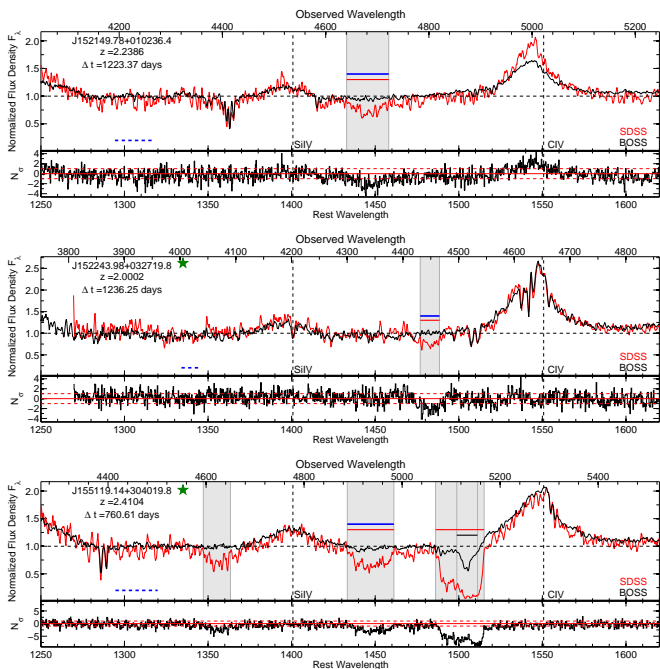


FIG. 3.— Multi-epoch spectra of quasars with disappearing BAL troughs obtained from SDSS-I/II (red) and BOSS (black). The  $x$ -axes show observed (top) and rest-frame (bottom) wavelengths in  $\text{\AA}$ . The dashed vertical lines show the emission-line rest wavelengths of Si IV  $\lambda\lambda$  1393, 1402 and C IV  $\lambda\lambda$  1548, 1550. BALs are shown as shaded areas, and the red and black horizontal lines indicate BALs in the same color as the corresponding spectra. Solid blue bars show disappearing BAL troughs, and dashed blue bars show wavelengths of corresponding Si IV velocities. Quasars with a green star next to their names are the ones that are identified as “pristine” examples of BAL disappearances (see §3.3). The lower section of each panel shows the  $N_\sigma$  values for SDSS vs. BOSS observations (black). The dashed horizontal lines show the  $\pm 1\sigma$  level.

our upper limits are conservative in that we do not allow for any narrowing of the absorption profile as it becomes weaker; analysis of our full BAL sample shows that such narrowing is typical.

We found that there are a few additional arguable cases of BAL disappearance that do not satisfy our formal definition for disappearing BAL troughs. Examples of such cases include J083817.00+295526.5, J092444.66–000924.1, J115244.20+030624.4, and J131010.07+052558.8. The first three of these arguable cases arise because of difficulties in deciding if a BAL trough should be split into two distinct components (one of which disappears) or not; in such cases we follow the formal BAL definition criteria associated with Equation 1. The fourth case arises from a C IV BAL lying close to the Si IV emission line; in this case separation of continuum vs. line emission is difficult.

We have investigated the Si IV absorption at velocities corresponding to disappearing C IV troughs. A total of 12 of 19 quasars have spectral coverage at the corresponding velocities in both the SDSS and the BOSS spectra. Two quasars (J004022.40+005939.6 and J081102.91+500724.2) show Si IV absorption at the corresponding velocity, and this absorption disappeared in the BOSS spectra for both of these quasars (see Figure 3).

We have investigated the Mg II and Al III regions of the 19 quasars with disappearing BAL troughs. All BOSS spectra have full coverage of the Mg II region, as do SDSS spectra in all but two cases (J004022.40+005939.6 and J134544.55+002810.7). None of the quasars with disappearing BAL troughs shows the presence of BALs in the Mg II or

Al III regions in their SDSS or BOSS spectra. Thus, certainly 17 and likely all 19 of these quasars are high-ionization BAL quasars.

Figure 4 shows the spectra of the six quasars with more than two epochs of observation: J004022.40+005939.6, J081102.91+500724.2, J085904.59+042647.8, J132216.24+052446.3, J134544.55+002810.7, and J155119.14+304019.8. Note the consistency of the BOSS spectra across the multiple epochs, which confirms the BAL disappearance and the general robustness of our analyses.

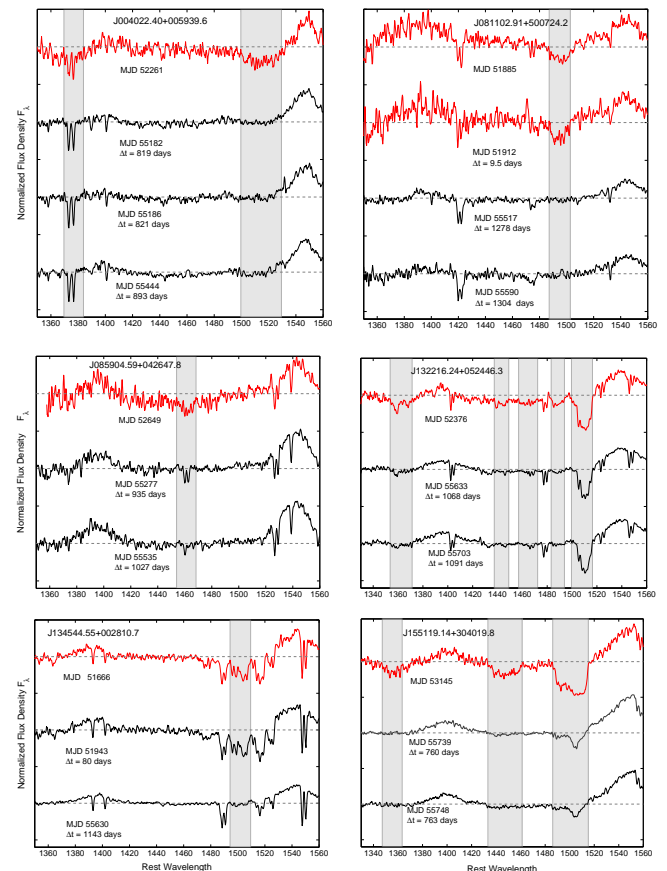


FIG. 4.— Multi-epoch observations of the six quasars with disappearing BAL troughs that have more than one SDSS or BOSS spectrum. Continuum-normalized SDSS (red) and BOSS (black) spectra are shown ordered by observation date. MJD values for each observation and the rest-frame time interval since the first observation are indicated under each spectrum. Horizontal dashed lines show continuum levels for each spectrum, the thick marks on the  $y$ -axis show the zero level for each spectrum, and shaded areas indicate BAL troughs.

### 3.4. Notes on Specific Objects

Here we describe the objects with remarkable properties or complex absorption spectra. Our descriptions supplement the objective approach adopted in §3.3 given the previously noted challenges sometimes associated with quantifying BAL troughs.

**J074650.59+182028.7:** Both of the NAL doublets that are blended with the disappearing C IV BAL trough are identified as C IV absorption in the BOSS NAL database (Lundgren et al. 2012).

**J085904.59+042647.8:** The NAL doublet that is blended with the disappearing C IV BAL trough is identified as C IV absorption (Lundgren et al. 2012). Figure 4 shows the three

available epochs of observation for this quasar where the NAL appears to vary between two BOSS spectra (corresponding to a significance level of 95%) separated by 92 days in the rest frame. This apparent variability, combined with the location of this NAL within a BAL, suggest that the NAL is not an intervening absorption system at a lower redshift than the quasar but arises in gas outflowing from the quasar.

*J093418.28+355508.3*: The SDSS spectrum of this quasar shows an adjacent absorption feature blueward (between rest-frame 1416–1421 Å) of the disappearing C IV BAL trough. This feature could be a distinct mini-BAL trough or the continuation of a BAL trough that was truncated in our formal approach owing to statistical fluctuations. Since this feature also disappears in the BOSS spectrum, its nature does not affect the interpretation of a BAL disappearance.

In the BOSS spectrum there is weak residual absorption that fails our formal definition (see §3.2 and especially Equation 1) for being a BAL or mini-BAL.

*J093620.52+004649.2*: According to Lundgren et al. (2007), the C IV BAL trough of this object emerged over a period of  $\leq 105.6$  days in the rest frame between two SDSS observations; the possible C IV absorption present in the first SDSS epoch does not qualify as a BAL. We now find that this same trough has disappeared over a period of  $\leq 3.3$  yr, and no remaining C IV absorption of any kind is apparent in the BOSS spectrum. Figure 5 shows the C IV BAL trough region in all three epochs. To our knowledge, this is the only reported example of a combined emergence and disappearance event for a BAL trough.

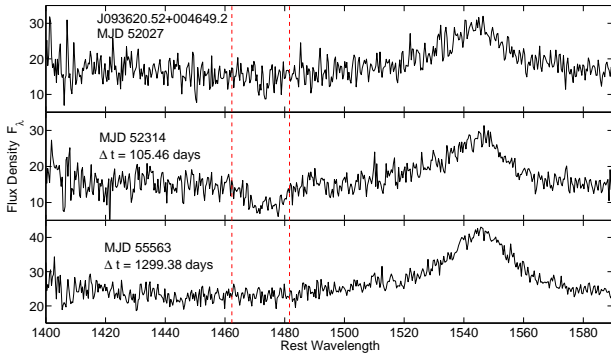


FIG. 5.— Three-epoch observations of *J093620.52+004649.2* that show the only reported example of a combined emergence and disappearance event for a BAL trough. The BAL trough of this object emerged between two SDSS observations (top and middle panels; Lundgren et al. 2007) and disappeared in the BOSS spectrum (bottom panel). The dashed red lines show the BAL trough region.

*J094806.58+045811.7*: The disappearing BAL trough in this case is clearly distinct from the non-disappearing trough at higher velocity. The two troughs are separated by 22 pixels ( $\approx 1500$  km s<sup>-1</sup>), 12 of which lie above the 90% continuum threshold (see §3.2). In fact, 6 pixels even lie above the continuum level.

*J104841.02+000042.8*: The NAL doublet that is blended with the weak disappearing C IV BAL trough is identified as C IV absorption (Lundgren et al. 2012).

*J112602.81+003418.2*: In the BOSS spectrum there is weak residual absorption that fails our formal definition for being a BAL or mini-BAL.

*J132216.24+052446.3*: In the BOSS spectrum there is weak residual absorption that fails our formal definition for being a BAL or mini-BAL.

*J133152.19+051137.9*: The disappearing C IV BAL trough is formally separated from the adjacent BAL trough at lower outflow velocities according to our BAL identification criteria. However, it is possible that there is some degree of physical connection between these two absorption systems. If they are indeed significantly connected, this would undermine the evidence for BAL disappearance in this quasar. It is notable, as apparent from the  $N_\sigma$  residuals in Figure 3, that the lower velocity BAL trough does not vary significantly as the higher velocity BAL trough disappears; this is suggestive of a lack of physical connection between these two systems. Further observations of this quasar are required for clarification.

*J133211.21+392825.9*: In the BOSS spectrum there is weak residual absorption that fails our formal definition for being a BAL or mini-BAL.

*J134544.55+002810.7*: This is the most complex, as well as the strongest, absorption system in our sample of disappearing BALs. In the SDSS spectrum, the disappearing BAL trough appears to be attached to a strong higher velocity C IV NAL doublet (see Lundgren et al. 2012) as well as a lower velocity mini-BAL. After the disappearance of the BAL trough, the NAL remains while the mini-BAL transforms to a NAL. Even if we consider the NAL, BAL and mini-BAL together as a connected BAL complex, the complex would still be listed as a disappearing BAL (since the only remaining features in the BOSS spectrum are NALs; see §3.3). We also note that there is another potentially connected mini-BAL at 1470–1485 Å in the SDSS spectrum; this mini-BAL disappears in the BOSS spectrum.

*J142132.01+375230.3*: In the BOSS spectrum there is weak residual absorption that fails our formal definition for being a BAL or mini-BAL.

*J142140.27–020239.0*: In the BOSS spectrum there is weak residual absorption that fails our formal definition for being a BAL or mini-BAL.

*J152149.78+010236.4*: In the BOSS spectrum there is weak residual absorption that fails our formal definition for being a BAL or mini-BAL.

#### 4. STATISTICAL PROPERTIES OF DISAPPEARING BALs

##### 4.1. How Common is BAL Disappearance?

The disappearance of BAL troughs is expected to be a rare event (e.g., Gibson et al. 2008; Hall et al. 2011). We have investigated 925 distinct BAL troughs in 582 quasars observed over 1.1–3.9 yr in the rest frame. From this sample, we have identified  $N_{dt} = 21$  disappearing BAL troughs in  $N_{qdt} = 19$  distinct quasars. Thus, on the observed timescales,  $f_{disapp} = 2.3^{+0.6}_{-0.5}\%$  (i.e., 21/925) of BAL troughs disappear, and  $f_{quasar} = 3.3^{+0.9}_{-0.7}\%$  (i.e., 19/582) of BAL quasars show a disappearing trough (quoted error bars are at  $1\sigma$  confidence following Gehrels 1986). If we consider only the pristine-sample objects defined in §3.3, the observed fraction of disappearing C IV BAL troughs is  $f_{disapp} = 1.2^{+0.6}_{-0.5}\%$  (i.e., 11/925) and the fraction of BAL quasars showing a disappearing trough is  $f_{quasar} = 1.9^{+0.8}_{-0.6}\%$  (i.e., 11/582). Table 3 lists the stated percentages above and the other quantities introduced below both for the standard sample and the pristine sample.

One potential implication of the observed frequency of disappearing C IV BAL troughs is a relatively short average trough rest-frame lifetime  $\bar{t}_{trough} \approx \langle \Delta t_{max} \rangle / f_{disapp} = 109^{+31}_{-22}$  yr, where  $\langle \Delta t_{max} \rangle$  is the average of the maximum time between observation epochs in a sample of BAL quasars (2.5 yr in this case) and



$f_{\text{disapp}}$  is the fraction of troughs that disappear over that time (also see Table 3). Here we state the average trough lifetime and average maximum observation time with different notations indicating that  $\bar{t}_{\text{trough}}$  is inferred, whereas  $\langle \Delta t_{\text{max}} \rangle$  is measured. Note that by lifetime we mean the time over which a trough is seen along our line of sight and not necessarily the lifetime of the gas clouds responsible for the absorption. The BAL phenomenon can last longer than  $\bar{t}_{\text{trough}}$  if troughs come and go along our line of sight within BAL quasars. If many troughs have extremely long lifetimes then the above is only a lower limit on the true  $\bar{t}_{\text{trough}}$ . In that case, the fraction  $f_{\text{short}}$  of relatively short-lived troughs that dominate the parent population of disappearing troughs must have lifetimes of only  $f_{\text{short}} \bar{t}_{\text{trough}}$ . Thus, we conclude that a significant fraction of BAL troughs have average lifetimes of a century or less.

Notably, our sample includes  $N_{\text{transform}} = 10$  examples of objects that have apparently transformed from BAL to non-BAL quasars; these are denoted in Table 1. BOSS spectra of these objects demonstrate that their C IV and Si IV regions do not have any remaining BAL (or mini-BAL) troughs.<sup>16</sup> Only two of these 10 objects (J004022.40+005939.6 and J152149.78+010236.4) have BOSS spectral coverage of the corresponding Ly $\alpha$  and N V BAL transitions as well, and visual inspection confirms that these spectra do not show any remaining BAL or mini-BAL troughs in Ly $\alpha$  or N V (see Figure 6).<sup>17</sup> As we are not aware of any BAL quasars that show convincing Ly $\alpha$  or N V absorption without also showing C IV or Si IV absorption, we consider the lack of remaining absorption in the latter transitions alone to be credible evidence of transformation from a BAL to a non-BAL quasar.<sup>18</sup> The one qualification here is that it is possible, in principle, that some of these objects could have transitioned to a very high-ionization BAL state like that seen in SBS 1542+541 (Telfer et al. 1998); SBS 1542+541 shows strong O VI absorption but only weak or no absorption in transitions like C IV, Si IV, and N V. However, we consider this an unlikely possibility because such very high-ionization BAL quasars appear to be rare based on a visual search of the spectra of high-redshift SDSS DR7 catalog (Schneider et al. 2010) quasars (by P.B.H.) and on their absence as contaminants in searches for damped Ly $\alpha$  absorption systems in the same catalog (J.X. Prochaska 2011, personal communication). The fraction of BAL quasars transforming to non-BAL quasars is  $f_{\text{transform}} = 1.7_{-0.5}^{+0.7}\%$  (i.e., 10/582) on 1.1–3.9 yr timescales. These are the first reported examples of BAL to non-BAL quasar transformations; the four previously reported BAL disappearance events described in §1 did not involve transformations from BAL to non-BAL quasar status (i.e., troughs from other ions or additional C IV troughs remained in the spectra).

These BAL to non-BAL quasar transformations set a lower limit on the lifetime of the ultraviolet BAL phenomenon along our line of sight of  $\bar{t}_{\text{BAL}} \simeq \langle \Delta t_{\text{max}} \rangle / f_{\text{transform}} = 150_{-50}^{+60}$  yr. However, defining the lifetime of the BAL phase along our

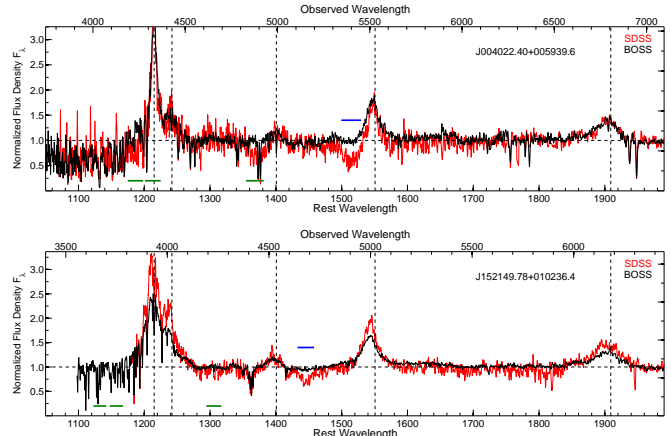


FIG. 6.— BAL quasars J004022.40+005939.6, J133211.21+392825.9, and J152149.78+010236.4 that transformed to non-BAL quasars after the disappearance of the C IV BAL trough (marked with a blue bar). Green bars under each spectrum indicate the velocities in the Ly $\alpha$ , N V, and Si IV regions corresponding to the disappearing C IV trough. Vertical dashed lines indicate the emission lines for Ly $\alpha$ , N V, Si IV, C IV, and C III, respectively, from left to right.

line of sight is more complicated than defining a trough lifetime along our line of sight. For example, if a BAL quasar has its only trough disappear but then has a different trough appear a year later, should this event be considered separate BAL phases or one phase with patchy absorption? Monitoring the strong X-ray absorption which is also characteristic of BAL quasars (e.g., Gallagher et al. 2002, 2006) would improve our understanding of how connected UV absorption variability is to absorption variability at other wavelengths, and thus to variability between BAL and non-BAL phases along a given line of sight, all of which can help test BAL outflow models.

#### 4.2. Luminosities, Black-Hole Masses, Reddening, and Radio Properties of Quasars with Disappearing BAL Troughs

In Figure 7, we compare our main-sample quasars to quasars with disappearing troughs in a plot of redshift versus absolute  $i$ -band magnitude ( $M_i$ ). We physically expect that, since the sampled rest-frame timescales are shortened toward higher redshifts, less BAL variability will be seen with increasing redshift. Therefore, we applied the two-sample Kolmogorov-Smirnov (K-S) test to compare  $M_i$  distributions for quasars with disappearing BAL troughs and the main-sample quasars sampled on similar rest-frame timescales (i.e.,  $z \leq 2.6$ ). We find no evidence that BAL quasars with disappearing troughs have exceptional  $M_i$  values compared to the main-sample quasars with similar redshifts (K-S probability of 68%). In addition, we compared SMBH mass estimates from Shen et al. (2011) for quasars with disappearing BAL troughs and our main-sample quasars. The quasars with disappearing C IV BAL troughs do not show any remarkable inconsistency from the main sample (K-S probability of 9% for  $z \leq 2.6$  quasars). Thus, the disappearing trough phenomenon appears to be generally present throughout the BAL quasar population.

We have also investigated if our quasars with disappearing C IV BAL troughs show any difference in intrinsic reddening from the main sample. Following G09, we have calculated a basic “reddening parameter”, defined as the ratio of the continuum flux densities at 1400 Å and 2500 Å. We do not detect any difference in the distributions of this parameter for the quasars with disappearing C IV BAL troughs and the main sample.

<sup>16</sup> Two of these objects, J114546.22+032251.9 and J152149.78+010236.4, do have strong multiple NAL systems in their BOSS spectra that do not overlap in velocity with the disappearing C IV BAL trough.

<sup>17</sup> The BOSS spectrum of J133211.21+392825.9 shows intervening absorption from a damped Ly $\alpha$  absorber that is not related to the BAL phenomenon. The intervening nature of this absorption is supported by its narrow width and symmetric shape, as well as by the fact that the maximum depth of the line is consistent with zero flux.

<sup>18</sup> One possible counterexample is the remarkable quasar PDS 456 which may show only broad Ly $\alpha$  absorption (O’Brien et al. 2005). However, the identification of the single broad absorption feature found in the spectrum of this quasar is not clear; e.g., it could be from highly blueshifted C IV.

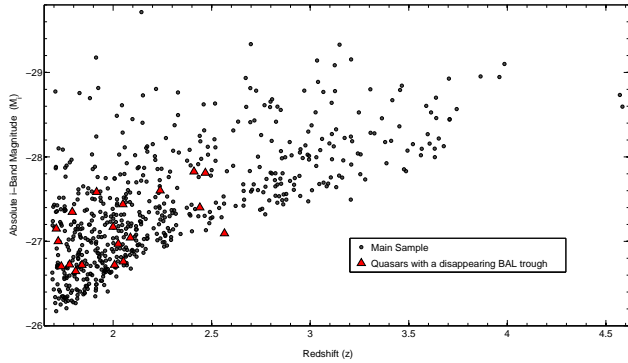


FIG. 7.— Redshifts vs. absolute  $i$ -band magnitudes of main-sample quasars in this study (black solid circles) and quasars with disappearing C IV BAL troughs (red triangles). Redshifts are from Hewett & Wild (2010), and  $M_i$  values are from Shen et al. (2011).

The FIRST survey has detected radio emission from two of the quasars with disappearing troughs. J004022.40+005939.6 is radio intermediate with  $R = 60.7$  and J081102.91+500724.2 is radio loud with  $R = 223.8$ . The quasars without detected radio emission have  $R < 5$  and are thus radio quiet. The BAL variability of radio-loud BAL quasars is not well understood and is just now being studied systematically (e.g., Miller et al. 2012). Our results for J004022.40+005939.6 and J081102.91+500724.2 demonstrate that BAL disappearance is a phenomenon of both radio-loud and radio-quiet quasars.

#### 4.3. EWs, Depths, Velocities, and Widths of Disappearing BAL Troughs

We have investigated the characteristics of disappearing C IV BAL troughs by comparing them with non-disappearing ones. Figure 8 shows a comparison of the EW distributions for disappearing BAL troughs, the other BAL troughs present in quasars that show one disappearing trough (i.e., those that do not disappear; see §4.4 for further discussion), and all 925 distinct BAL troughs in the main sample. In order to be consistent, we measured the BAL-trough parameters from the observations obtained at epoch  $t_1$  (i.e., the latest observation from the SDSS). The K-S test results show that there is only a 0.09% chance of consistency between the EW distributions of disappearing BAL troughs and all main-sample BAL troughs. Based on this result and Figure 8, it appears that BAL disappearance tends to occur for weak or moderate-strength absorption troughs but not the strongest ones. In particular, no troughs with  $EW > 12 \text{ \AA}$  disappeared. Furthermore, the K-S test results comparing the main-sample C IV BAL troughs and the additional non-disappearing C IV BAL troughs defined in §4.4 show no evidence for inconsistency (K-S probability of 56.9%).

Figure 9 shows the distributions of the BAL-trough depth parameter,  $f_{\text{deep}}^{25}$ , for disappearing BAL troughs and for all 925 distinct BAL troughs in the main sample. The K-S test shows that these two distributions only have a 0.03% chance of consistency. The BAL troughs that disappear are shallower than BAL troughs in general, although some fairly deep BAL troughs do disappear.

Figures 10a and 10b show the distributions of  $v_{\text{max}}$  and  $v_{\text{min}}$  (see §3.2) for disappearing and all 925 distinct C IV BAL troughs in the main sample. The  $v_{\text{max}}$  distribution of all BALs shows that this quantity is roughly distributed evenly between  $-3000$  and  $-25000 \text{ km s}^{-1}$ , while the corresponding  $v_{\text{min}}$  distribution rises toward low velocities. The peak in the  $v_{\text{min}}$

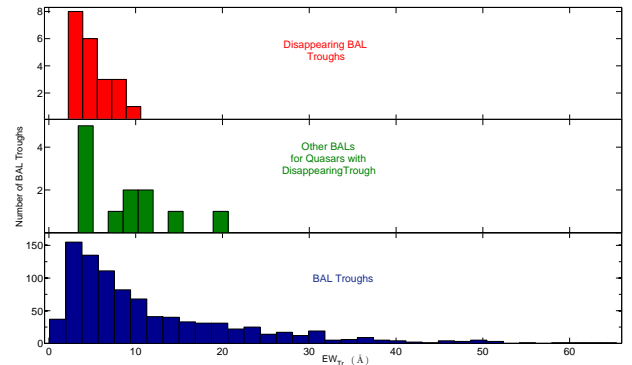


FIG. 8.— EW distributions for disappearing C IV BAL troughs (upper panel, red), the other BAL troughs present in quasars that show one disappearing trough (middle panel, green), and all 925 distinct C IV BAL troughs in the main sample (lower panel, blue).

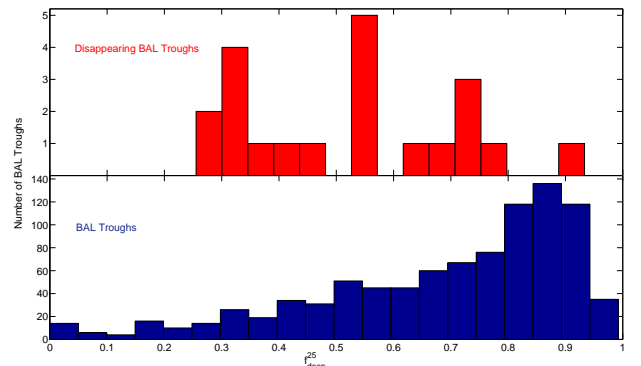


FIG. 9.— Distribution of  $f_{\text{deep}}^{25}$  for disappearing C IV BAL troughs (upper panel) and for all 925 distinct C IV BAL troughs in the main sample (lower panel).

distribution around  $-3000 \text{ km s}^{-1}$  is artificially elevated due to the assigned lower velocity limit. The distribution histograms in Figures 10a and 10b show basic agreement with the similar distributions presented in G09 (see their Figure 8), although the  $v_{\text{max}}$  and  $v_{\text{min}}$  values in G09 give the velocities for all BALs together in a given spectrum. A K-S test for the  $v_{\text{max}}$  distributions of disappearing BAL troughs and all main-sample BAL troughs shows that these two distributions are not demonstrably inconsistent (K-S probability of 11.1%), while the corresponding test using the  $v_{\text{min}}$  distributions gives a probability of 0.1%. Based on this result and Figures 10a and 10b, it appears that BAL disappearance tends to occur for BAL troughs with relatively high values of  $v_{\text{min}}$ ; this result indicates that our requirement of trough detachment (see §2.2) should not cause significant biases to our sample statistics.

Figures 10c and 10d show the distributions of the central velocity [ $v_c = (v_{\text{max}} + v_{\text{min}})/2$ ] and trough width ( $\Delta v = |v_{\text{max}} - v_{\text{min}}|$ ) for disappearing and all 925 distinct C IV BAL troughs in the main sample. A K-S test yields a probability of 1.5% for consistency between the two  $v_c$  distributions, indicating that disappearing BALs tend to have higher outflow central velocities than BALs in general. A K-S test for the  $\Delta v$  distributions of disappearing BAL troughs and all main-sample BAL troughs shows that these two distributions have a 6.9% chance of consistency. These distributions suggest that disappearing BAL troughs tend to be narrower than the average BAL troughs.

According to our statistical tests above, C IV BAL disappearance generally occurs for weaker troughs as well as

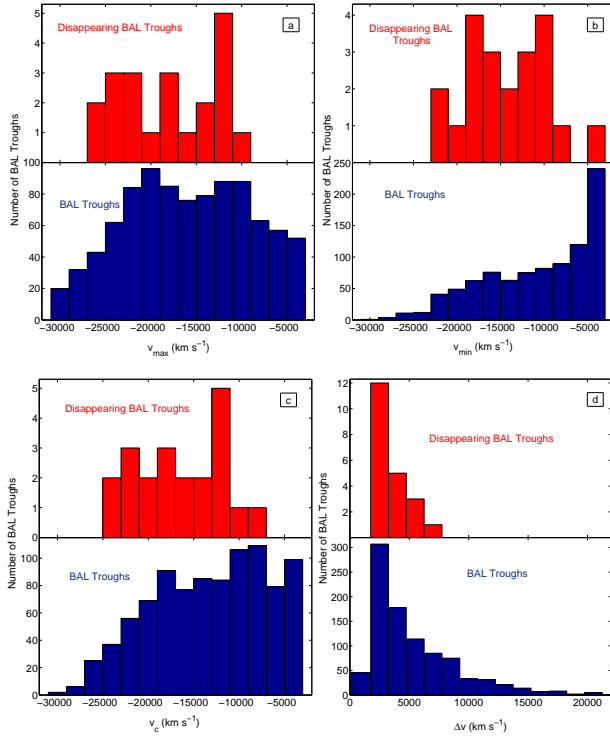


FIG. 10.—  $v_{\max}$  (a),  $v_{\min}$  (b),  $v_c$  (c), and  $\Delta v$  (d) distributions for disappearing C IV BAL troughs (upper panels), and all 925 distinct C IV BAL troughs in the main sample (lower panels).

higher velocity troughs. It is possible that these two results are related, or that one is simply the effect of the other. For example, in our main sample we find that weak BAL troughs can generally achieve higher velocities than strong BAL troughs (although there is a wide range of velocity observed at all trough strengths); as a result, the average velocity for the population of weak BAL troughs is higher than that for strong BAL troughs. This basic result has also been noted by others (e.g., G09; Capellupo et al. 2011). Thus, the tendency for BAL disappearance to occur for weaker troughs could also lead to disappearing troughs having higher velocities, on average, than for the whole trough population. A larger sample of disappearance events will be required to determine if BAL strength or BAL velocity, if either, is primarily connected to BAL disappearance.

#### 4.4. Connections Between Disappearing and Non-Disappearing Troughs

Multiple troughs in the quasar spectra that have at least one disappearing BAL can be used to investigate connections between disappearing and non-disappearing troughs. Among the 19 quasars with disappearing troughs, we find nine that have at least one additional C IV BAL trough that does not disappear (J093418.28+355508.3, J094806.58+045811.7, J104841.02+000042.8, J112602.81+003418.2, J132216.24+052446.3, J133152.19+051137.9, J134544.55+002810.7, J142140.27–020239.0, and J155119.14+304019.8). These nine quasars contain a total of 12 C IV troughs that do not disappear and satisfy the criteria in §2.2. We will hereafter refer to these as the “additional non-disappearing C IV troughs”. Figure 11 compares the EWs at two epochs,  $t_1$  and  $t_2$ , for distinct C IV BAL troughs in the main sample and the additional non-disappearing C IV troughs. The additional non-disappearing C IV troughs

almost always weaken (by up to 85%), except for the least blueshifted trough of J133152.19+051137.9, which strengthens by 7%. In J094806.58+045811.7, J104841.02+000042.8, J134544.55+002810.7, and J142140.27–020239.0, the additional non-disappearing C IV trough transforms from a BAL to a mini-BAL as it weakens. The weakening of the additional non-disappearing C IV troughs is statistically significant, given that the combinatorial probability to have 11 or more troughs out of 12 weaken is only 0.3%. The fact that the additional non-disappearing troughs usually weaken indicates that variability across multiple troughs is coordinated.

Figure 12 shows fractional EW variations for the 12 additional non-disappearing C IV troughs versus central velocity offset from the disappearing trough. The error bars on EW fractional changes are calculated from the EW uncertainties at the two epochs (i.e.,  $t_1$  and  $t_2$ ). Notably, the coordinated variability across multiple troughs persists even for velocity offsets as large as 10000–15000  $\text{km s}^{-1}$ . This result is even more remarkable given that BAL troughs often vary in discrete regions only a few thousand  $\text{km s}^{-1}$  wide (Gibson et al. 2008), and it requires further investigation.

In Figure 12 nine of the 12 additional non-disappearing C IV troughs have smaller velocities than the disappearing C IV troughs. This result implies that, for BAL quasars showing multiple troughs, the highest velocity trough is usually the one that disappears. This suggestive result is not clearly significant in the current sample, with a combinatorial probability of chance occurrence of 7%, and it needs further investigation.

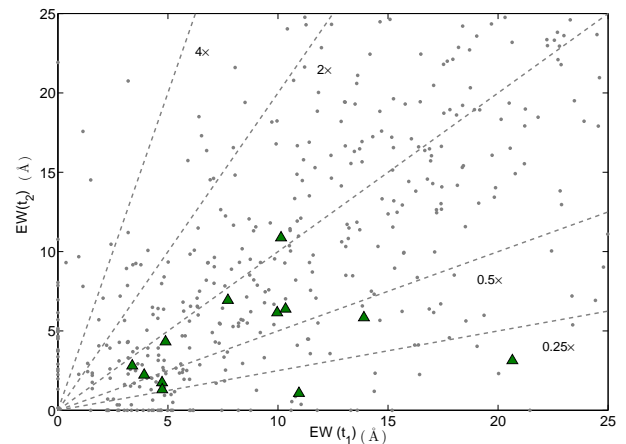


FIG. 11.— The EWs at two epochs for all BAL troughs in the main sample (grey circles). The green triangles mark the other BAL troughs present in quasars that show one disappearing trough; note that in all cases but one the other BAL troughs weaken. Dashed lines indicate four times, two times, one-half of, and one-quarter of the first-epoch EWs, from top to bottom.

We also investigated Si IV BAL troughs at velocities that correspond to one of the additional non-disappearing C IV troughs. The additional Si IV BAL troughs that are found in the spectra of three quasars show dramatic variations; the Si IV BAL troughs in J132216.24+052446.3 and J142140.27–020239.0 transform to mini-BALs (weakening in EW by 88% and 87%, respectively), and the trough in J155119.14+304019.8 disappears.

The results above demonstrate that outflow stream lines separated by large velocities apparently can either coordinate their variability or are being acted upon by some external

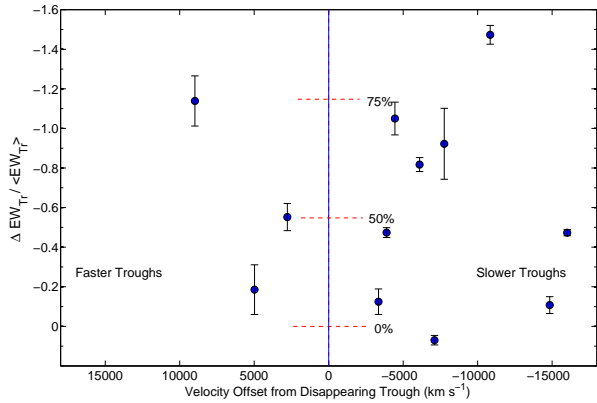


FIG. 12.— Fractional changes in EW for 12 additional non-disappearing C IV BAL troughs present in quasars that show one disappearing trough. The  $x$ -axis is the central velocity  $[(v_{\max} + v_{\min})/2]$  of each trough relative to that of the trough that disappeared. The horizontal dashed red lines indicate the levels for 50%, 75%, and 0% decrease in trough strength. Note that even BAL troughs separated by 10000–15000  $\text{km s}^{-1}$  from the disappearing troughs weaken, showing coordinated variations over a large velocity range.

agent that enforces coordination. The latter possibility appears more likely given understanding of BAL winds. One example of an external agent could be disk rotation. Such rotation might lead to coordinated observed changes in absorption by several non-axisymmetric outflows that are loosely anchored to the accretion disk at different radii, provided there is some large-scale azimuthal asymmetry of the disk similarly affecting several stream lines. Another possible external agent could be the “shielding gas” that prevents BAL outflows from being overionized by highly energetic emission generated close to the SMBH (e.g., Murray et al. 1995; Proga et al. 2000). This shielding gas is found to be variable in wind simulations (e.g., Sim et al. 2010), and the limited long-term X-ray variability observations show rare apparent examples of shielding-gas variations (e.g., Saez et al. 2012). Variations of the shielding gas could change the level of ionizing-continuum radiation reaching larger radii. In response to these changes in ionizing continuum, several absorption components at different velocities could rise and fall in ionization level together with some features disappearing. One challenge for this scenario is that BAL-trough variations generally do not appear to be correlated with variations of the observable continuum (see §1). However, since the observable continuum is typically that longward of Ly $\alpha$ , it is perhaps possible that the ionizing continuum at shorter wavelengths varies differently in at least some cases.

## 5. SUMMARY AND FUTURE WORK

We have used a systematically observed sample of 582 BAL quasars with 925 distinct C IV BAL troughs to provide the first statistically meaningful constraints upon BAL disappearance on multi-year timescales. Our main results are the following:

1. We have identified 21 cases of C IV BAL disappearance in 19 quasars. On rest-frame timescales of 1.1–3.9 yr,  $f_{\text{disappear}} = 2.3_{-0.5}^{+0.6}\%$  of BAL troughs disappear and  $f_{\text{quasar}} = 3.3_{-0.7}^{+0.9}\%$  of BAL quasars show a disappearing trough. If we consider only the pristine sample defined in §3.3, then we find 11 cases of C IV BAL disappearance in 11 quasars; the corresponding percentages are  $f_{\text{disappear}} = 1.2_{-0.4}^{+0.4}\%$  and  $f_{\text{quasar}} = 1.9_{-0.6}^{+0.8}\%$ . See §4.1.
2. The observed frequency of disappearing C IV BAL

troughs suggests an average trough rest-frame lifetime of 100–200 yr. See §4.1.

3. Ten quasars showing C IV BAL disappearance have apparently transformed from BAL to non-BAL quasars; these are the first reported examples of such transformations. The frequency of BAL to non-BAL quasar transformation on timescales of 1.1–3.9 yr is  $1.7_{-0.5}^{+0.7}\%$ . See §4.1.
4. The BAL quasars with disappearing troughs have representative luminosities ( $M_i$  values), SMBH mass estimates, and intrinsic reddening compared to our sample as a whole. See §4.2.
5. As expected from the fact that most BAL quasars are radio quiet, most BAL quasars with disappearing troughs are radio quiet. However, we do find one such quasar that is radio loud and another that is radio intermediate. Thus, BAL disappearance is a phenomenon of both radio-quiet and radio-loud quasars. See §4.2.
6. BAL disappearance appears to occur mainly for weak or moderate-strength absorption troughs but not the strongest ones; e.g., no troughs with  $\text{EW} > 12 \text{ \AA}$  disappeared. The BAL troughs that disappear are shallower than BAL troughs in general, although some fairly deep BAL troughs do disappear. See §4.3.
7. Disappearing C IV BAL troughs show higher outflow velocities than BAL troughs in general, as indicated by their measured central velocities and minimum velocities (though their measured maximum velocities do not appear exceptional). There is also suggestive evidence that disappearing BAL troughs tend to be narrower than BAL troughs in general. This tendency for BAL disappearance to occur for higher velocity troughs could be related to, or even a secondary effect of, the fact that BAL disappearance appears to occur mainly for weak or moderate-strength absorption troughs (see point 5 above). See §4.3.
8. When one BAL trough in a quasar spectrum disappears, the other present troughs usually weaken (11 times out of 12 in our sample, corresponding to a significance level  $> 99\%$ ). The phenomenon occurs even for velocity offsets as large as 10000–15000  $\text{km s}^{-1}$ . Variability across multiple troughs appears surprisingly coordinated. Possible causes of such coordinated variations could be disk-wind rotation or variations of shielding gas that lead to variations of ionizing-continuum radiation. These possible agents will need to be considered in future models of quasar winds. See §4.4.

Given the results above, we can identify several promising observational projects that should extend understanding of BAL disappearance. Further spectroscopy of the quasars that have shown BAL disappearance will allow a search for reappearance of any of these BALs. Such reappearances at the same measured velocities would not be expected if wind stream lines have moved out of the line of sight owing to rotation of a non-axisymmetric outflow. However, BAL reappearance should be possible if the disappearance is a consequence of BAL weakening to strengths below our detection threshold.

Systematic large-sample variability studies should let us assess the extent to which BAL disappearance is just the extension of normal BAL variability down to very small EWs. Further spectroscopy will also allow monitoring of the additional non-disappearing troughs. Furthermore, the planned absolute flux calibration of the BOSS spectra (e.g., Margala & Kirkby 2011) will allow a search for any systematic continuum-level changes associated with BAL disappearance. The rate of BAL emergence events must balance that of BAL disappearance events if the BAL quasar population is in a steady state, and thus systematic large-scale studies of BAL emergence will be a critical complement to those of disappearance. Finally, multiwavelength observations of the quasars showing BAL disappearance are worthwhile. For example, X-ray observations of objects that have transformed from BAL to non-BAL quasars will be able to assess if the X-ray absorbing shielding gas is still present along the line of sight.

The main-sample data set utilized in this study, along with the still incoming BOSS observations, will be effective for a variety of additional investigations of BAL variability. These include studies of (1) absorption EW variability as a function of timescale for different BAL transitions, (2) connections between BAL, emission-line, and reddening variability, and (3) the effects of luminosity, redshift, SMBH mass, Eddington fraction, and radio properties on BAL variability.

We gratefully acknowledge financial support from National Science Foundation grant AST-1108604 (NFA, WNB,

DPS) and from NSERC (PBH). We thank D. M. Capellupo and F. Hamann for sharing their EW measurements for the Capellupo et al. (2011) sample in Figure 1. We thank K. Dawson, M. Eracleous, D. Proga, and J. Wu for helpful discussions. We also thank the anonymous referee for useful feedback.

Funding for SDSS-III has been provided by the Alfred P. Sloan Foundation, the Participating Institutions, the National Science Foundation, and the U.S. Department of Energy Office of Science. The SDSS-III web site is <http://www.sdss3.org/>.

SDSS-III is managed by the Astrophysical Research Consortium for the Participating Institutions of the SDSS-III Collaboration including the University of Arizona, the Brazilian Participation Group, Brookhaven National Laboratory, University of Cambridge, Carnegie Mellon University, University of Florida, the French Participation Group, the German Participation Group, Harvard University, the Instituto de Astrofísica de Canarias, the Michigan State/Notre Dame/JINA Participation Group, Johns Hopkins University, Lawrence Berkeley National Laboratory, Max Planck Institute for Astrophysics, Max Planck Institute for Extraterrestrial Physics, New Mexico State University, New York University, Ohio State University, Pennsylvania State University, University of Portsmouth, Princeton University, the Spanish Participation Group, University of Tokyo, University of Utah, Vanderbilt University, University of Virginia, University of Washington, and Yale University.

## REFERENCES

- Aihara H., et al., 2011, *ApJS*, 193, 29 [erratum, *ApJS*, 195, 26]  
 Allen, J. T., Hewett, P. C., Maddox, N., Richards, G. T., & Belokurov, V. 2011, *MNRAS*, 410, 860  
 Anderson, L., et al. 2012, arXiv:1203.6594  
 Arav, N., Becker, R. H., Laurent-Muehleisen, S. A., Gregg, M. D., White, R. L., Brotherton, M. S., & de Kool, M. 1999, *ApJ*, 524, 566  
 Barlow, T. A. 1993, PhD thesis, Univ. of California  
 Becker, R. H., White, R. L., & Helfand, D. J. 1995, *ApJ*, 450, 559  
 Bevington, P. R., & Robinson, D. K. 2003, *Data Reduction and Error Analysis for the Physical Sciences* (3rd ed.; Boston, MA: McGraw-Hill)  
 Blandford, R. D., & Payne, D. G. 1982, *MNRAS*, 199, 883  
 Bolton, A. S., Burles, S., Schlegel, D. J., Eisenstein, D. J., & Brinkmann, J. 2004, *AJ*, 127, 1860  
 Capellupo, D. M., Hamann, F., Shields, J. C., Rodríguez Hidalgo, P., & Barlow, T. A. 2011, *MNRAS*, 413, 908  
 Capellupo, D. M., Hamann, F., Shields, J. C., Rodríguez Hidalgo, P., & Barlow, T. A. 2012, arXiv:1203.1051  
 Cardelli, J. A., Clayton, G. C., & Mathis, J. S. 1989, *ApJ*, 345, 245  
 Condon, J. J., Cotton, W. D., Greisen, E. W., Yin, Q. F., Perley, R. A., Taylor, G. B., Broderick, J. J., et al. 1998, *AJ*, 115, 1693  
 Crenshaw, D. M., Kraemer, S. B., & George, I. M. 2003, *ARA&A*, 41, 117  
 Eisenstein, D. J., et al. 2011, *AJ*, 142, 72  
 Gallagher, S. C., Brandt, W. N., Chartas, G., Priddey, R., Garmire, G. P., Sambruna, R. M., et al. 2006, *ApJ*, 644, 709  
 Gallagher, S. C., Brandt, W. N., Chartas, G., Garmire, G. P. 2002, *ApJ*, 567, 37  
 Ganguly, R., & Brotherton, M. S. 2008, *ApJ*, 672, 102  
 Gehrels, N. 1986, *ApJ*, 303, 336  
 Gibson, R. R., Brandt, W. N., Schneider, D. P., & Gallagher, S. C. 2008, *ApJ*, 675, 985  
 Gibson, R. R., et al. 2009, *ApJ*, 692, 758  
 Gibson, R. R., Brandt, W. N., Gallagher, S. C., Hewett, P. C., & Schneider, D. P. 2010, *ApJ*, 713, 220  
 Gunn, J. E., Siegmund, W. A., Mannery, E. J., et al. 2006, *AJ*, 131, 2332  
 Hall, P. B., Anderson, S. F., Strauss, M. A., et al. 2002, *ApJS*, 141, 267  
 Hall, P. B., Anosov, K., White, R. L., Brandt, W. N., Gregg, M. D., Gibson, R. R., Becker, R. H., & Schneider, D. P. 2011, *MNRAS*, 411, 2653  
 Hamann, F. 1998, *ApJ*, 500, 798  
 Hamann, F., & Sabra, B. 2004, in *ASP Conf. Ser. 311, AGN Physics with the Sloan Digital Sky Survey*, ed. G. T. Richards & P. B. Hall (San Francisco, CA: ASP), 203  
 Hamann, F., Kaplan, K. F., Rodríguez Hidalgo, P., Prochaska, J. X., & Herbert-Fort, S. 2008, *MNRAS*, 391, L39  
 Hewett, P. C. & Wild V. 2010, *MNRAS*, 405, 2302  
 Hewett, P. C., Foltz, C. B., & Chaffee, F. H. 1995, *AJ*, 109, 1498  
 Hopkins, P. F., et al. 2004, *AJ*, 128, 1112  
 Jukkariinen, V., Shields, G. A., Beaver, E. A., Burbidge, E. M., Cohen, R. D., Hamann, F., & Lyons, R. W. 2001, *ApJ*, 549, L155  
 Kaspi, S., et al. 2002, *ApJ*, 574, 643  
 King, A. R. 2010, *MNRAS*, 402, 1516  
 Krongold, Y., Binette, L., & Hernandez-Ibarra, F. 2010, *ApJ*, 724, 203  
 Leighly, K. M., Hamann, F., Casebeer, D. A., & Grupe, D. 2009, *ApJ*, 701, 176  
 Lundgren, B. F., Wilhite, B. C., Brunner, R. J., Hall, P. B., Schneider, D. P., York, D. G., Vanden Berk, D. E., & Brinkmann, J. 2007, *ApJ*, 656, 73  
 Lundgren, B. F., York, D. G., et al. (2012, in preparation)  
 Ma, F. 2002, *MNRAS*, 335, L99  
 Margala, D., Kirkby, D. 2011, in *SDSS BOSS QSO Workshop* (Princeton, NJ)  
 Miller, B. P., Welling, C. A., Brandt, W. N., & Gibson, R. R. 2012, *AGN Winds in Charleston* (Charleston, SC), arXiv:1201.2676  
 Murray, N., Chiang, J., Grossman, S. A., & Voit, G. M. 1995, *ApJ*, 451, 498  
 O'Brien, P. T., Reeves, J. N., Simpson, C., & Ward, M. J. 2005, *MNRAS*, 360, L25  
 Pei, Y. C. 1992, *ApJ*, 395, 130  
 Press, W.H., S.A. Teukolsky, W.T. Vetterling, and B.P. Flannery, 1992, *Numerical Recipes in C: The Art of Scientific Computing* (2nd ed.; New York, NY: Cambridge Univ. Press)  
 Proga, D., Kallman T. R., Drew, J. E., & Hartley, L. E. 2002, *ApJ*, 572, 382  
 Ross, N. P., et al. 2012, *ApJS*, 199, 3  
 Saez, C., Brandt, W. N., Gallagher, S. C., Bauer, F. E. & Garmire, G. P. 2012, *ApJ*, in press  
 Savitzky, A., & Golay, M.J.E. 1964, *Analytical Chemistry*, 36, 1627  
 Schlegel, D. J., Finkbeiner, D. P., & Davis, M. 1998, *ApJ*, 500, 525  
 Schneider, D. P., et al. 2007, *AJ*, 134, 102  
 Schneider, D. P., et al. 2010, *AJ*, 139, 2360  
 Shen, Y., et al. 2011, *ApJS*, 194, 45  
 Sim, S. A., Proga, D., Miller, L., Long, K. S., & Turner, T. J. 2010, *MNRAS*, 408, 1396  
 Springel, V., Di Matteo, T., & Hernquist, L. 2005, *MNRAS*, 361, 776  
 Telfer, R. C., Kriss, G. A., Zheng, W., Davidsen, A. F., & Green, R. F. 1998, *ApJ*, 509, 132

Vivek, M., Srianand, R., Mahabal, A., & Kuriakose, V. C. 2012, MNRAS, L403  
Weymann, R. J., Morris, S. L., Foltz, C. B., & Hewett, P. C. 1991, ApJ, 373, 23

White, R. L., et al. 2000, ApJS, 126, 133

TABLE 1  
SAMPLE OF QUASARS SHOWING DISAPPEARING BAL TROUGHS

SDSS Name	Redshift <sup>a</sup> $z$	$i^b$ (mag)	$M_i^c$ (mag)	Plate-MJD-Fiber <sup>d</sup>	BI <sup>e</sup> ( $\text{km s}^{-1}$ )	$N_{\text{Tr}}^f$
J004022.40+005939.6 <sup>‡</sup>	2.565±0.0006	19.223±0.027	−27.094	0690-52261-563	1668	1
				3587-55182-950	0	0
				3589-55186-558	0	0
				4222-55444-710	0	0
J074650.59+182028.7 <sup>†, ‡</sup>	1.9163±0.0005	18.043±0.016	−27.584	1582-52939-095	1241	1
				4492-55565-828	0	0
J081102.91+500724.2 <sup>‡</sup>	1.8422±0.0006	18.838±0.016	−26.720	0440-51885-377	591	1
				0440-51912-395	665	1
				3699-55517-062	0	0
				4527-55590-028	0	0
J085904.59+042647.8 <sup>†, ‡</sup>	1.8104±0.0005	18.812±0.022	−26.646	1192-52649-291	854	1
				3817-55277-538	0	0
				3814-55535-928	0	0
J093418.28+355508.3	2.4402±0.0007	18.902±0.016	−27.400	1275-52996-096	1621	2
				4575-55590-498	1007	1
J093620.52+004649.2 <sup>‡</sup>	1.7213±0.0005	18.391±0.016	−27.001	0476-52314-444	958	1
				3826-55563-542	0	0
J094806.58+045811.7	1.7371±0.0006	18.640±0.024	−26.704	0994-52725-288	2146	3
				4798-55672-934	317	1
J104841.02+000042.8 <sup>†</sup>	2.0263±0.0006	18.720±0.016	−26.970	0276-51909-310	2133	2
				3835-55570-398	0	0
J112602.81+003418.2	1.7928±0.0005	18.082±0.016	−27.348	0281-51614-432	2421	2
				3839-55575-844	1024	1
J114546.22+032251.9 <sup>‡</sup>	2.0075±0.0007	19.058±0.023	−26.721	0514-51994-458	389	1
				4766-55677-050	0	0
J132216.24+052446.3	2.0498±0.0006	18.384±0.019	−27.438	0851-52376-622	2903	4
				4761-55633-794	1154	1
				4839-55703-442	1125	1
				0852-52375-626	3840	3
J133152.19+051137.9	1.7118±0.0005	18.182±0.019	−27.150	4759-55649-756	3255	2
				2005-53472-330	690	1
J133211.21+392825.9 <sup>‡</sup>	2.0520±0.0009	19.021±0.023	−26.760	4708-55704-412	0	0
				0300-51666-426	1712	1
J134544.55+002810.7	2.4680±0.0005	18.535±0.019	−27.810	0300-51943-382	2875	1
				4043-55630-868	0	0
				1380-53084-013	854	1
J142132.01+375230.3 <sup>‡</sup>	1.7791±0.0006	18.658±0.019	−26.725	4712-55738-030	0	0
				0917-52400-546	3950	3
J142140.27−020239.0	2.0878±0.0006	18.877±0.016	−27.044	4032-55333-736	1002	1
				0313-51673-339	807	1
J152149.78+010236.4 <sup>‡</sup>	2.2386±0.0004	18.558±0.018	−27.602	4011-55635-166	0	0
				0592-52025-254	374	1
J152243.98+032719.8 <sup>‡</sup>	2.0002±0.0005	18.653±0.018	−27.172	4803-55734-442	0	0
				1580-53145-008	5176	2
J155119.14+304019.8	2.4104±0.0004	18.493±0.016	−27.826	5011-55739-054	417	1
				5010-55748-492	382	1

<sup>a</sup> Redshifts are from Hewett & Wild (2010), calculated from the cross correlation of the Mg II, C III], and C IV emission lines.

<sup>b</sup> The  $i$ -band magnitude given in the SDSS DR5 quasar catalog (Schneider et al. 2007).

<sup>c</sup> Absolute  $i$ -band magnitude from Shen et al. (2011).

<sup>d</sup> Unique Plate-MJD-Fiber numbers for each spectrum. BOSS spectra have  $\text{MJD} \geq 55176$  (see §4 of Ross et al. 2012).

<sup>e</sup> Balnicity index of each quasar in the given observation, summed over all troughs in the velocity range  $-3000 \leq v \leq -30000 \text{ km s}^{-1}$ . None of the quasars in the main sample has a disappearing BAL trough beyond this velocity range.

<sup>f</sup> Number of BAL troughs in each spectrum.

<sup>†</sup> Blended NAL(s) with disappearing BAL troughs.

<sup>‡</sup> Quasars that transformed from BAL to non-BAL quasars.

TABLE 2  
PARAMETERS OF DISAPPEARING BAL TROUGHS

Name SDSS	MJD <sup>a</sup>	EW ( $\text{\AA}$ )	$v_{\max}$ ( $\text{km s}^{-1}$ )	$v_{\min}$ ( $\text{km s}^{-1}$ )	$f_{\text{deep}}^{25}$ <sup>b</sup>	$\Delta t^c$ (days)	$\log(P_{\chi^2})^d$
J004022.40+005939.6	52261	10.60±0.705	-10067	-4167	0.74	819.35	< -300
J074650.59+182028.7 <sup>†</sup>	52939	8.76±0.212	-24994	-18015	0.46	900.46	< -300
J081102.91+500724.2	51912	4.70±0.477	-12405	-9830	0.74	1268.38	-8.59
J085904.59+042647.8 <sup>†</sup>	52649	5.22±0.476	-19315	-16370	0.73	935.10	-11.34
J093418.28+355508.3	52996	3.60±0.272	-25575	-21959	0.31	754.03	-13.79
J093620.52+004649.2	52314	6.15±0.373	-17603	-13677	0.68	1193.91	< -300
J094806.58+045811.7	52725	5.98±0.549	-21138	-16797	0.55	1076.69	-15.96
J104841.02+000042.8 <sup>†</sup>	51909	2.25±0.185	-12757	-10654	0.33	1209.73	-11.51
J112602.81+003418.2	51614	4.27±0.148	-26449	-22919	0.54	1418.29	< -300
J114546.22+032251.9	51994	3.34±0.328	-12771	-9682	0.28	1224.61	-11.60
J132216.24+052446.3	52376	2.72±0.184	-22727	-20322	0.38	1067.94	< -300
	52376	3.02±0.218	-18691	-15564	0.26	1067.94	-9.29
	52376	2.30±0.176	-13360	-11213	0.33	1067.94	-9.90
J133152.19+051137.9	52375	3.16±0.219	-12549	-10440	0.56	1207.32	< -300
J133211.21+392825.9	53472	4.68±0.349	-21377	-17861	0.53	731.32	-12.41
J134544.55+002810.7	51943	7.60±0.182	-11269	-8096	0.92	1063.15	< -300
J142132.01+375230.3	53084	5.15±0.343	-17005	-14193	0.76	954.99	< -300
J142140.27-020239.0	52400	4.55±0.177	-15968	-12922	0.57	949.87	< -300
J152149.78+010236.4	51673	6.03±0.460	-23658	-18462	0.41	1223.37	< -300
J152243.98+032719.8	52025	2.77±0.203	-14622	-12300	0.34	1236.25	< -300
J155119.14+304019.8	53145	8.20±0.428	-23588	-17834	0.64	760.61	< -300

<sup>a</sup> MJD of the observation used for BAL parameter measurements, which is taken to be the last SDSS observation that possesses the disappearing trough.

<sup>b</sup> Fraction of BAL bins which lie at least 25% under the continuum.

<sup>c</sup> The rest-frame time interval between the last observation that possesses the disappearing trough, given in column 2, and the first observation that shows disappearance.

<sup>d</sup> Logarithm of  $\chi^2$  probability which gives the probability of consistency between the SDSS and BOSS observations in the region limited by  $v_{\max}$  and  $v_{\min}$  (see §3.3).

<sup>†</sup> Blended NAL(s) with disappearing BAL troughs.

TABLE 3  
OBSERVED FRACTIONS AND LIFETIMES FOR DISAPPEARING BAL TROUGHS

	$N_{\text{dt}}^a$	$f_{\text{disapp}}^b$ (%)	$N_{\text{qdt}}^c$	$f_{\text{quasar}}^d$ (%)	$N_{\text{transform}}^e$	$f_{\text{transform}}^f$ (%)	$\bar{t}_{\text{trough}}^g$ (yr)	$\bar{t}_{\text{BAL}}^h$ (yr)
Standard Sample	21	2.3 <sup>+0.6</sup> <sub>-0.5</sub>	19	3.3 <sup>+0.9</sup> <sub>-0.7</sub>	10	1.7 <sup>+0.7</sup> <sub>-0.5</sub>	109 <sup>+31</sup> <sub>-22</sub>	150 <sup>+60</sup> <sub>-50</sub>
Pristine Sample	11	1.2 <sup>+0.5</sup> <sub>-0.4</sub>	11	1.9 <sup>+0.8</sup> <sub>-0.6</sub>	7	1.2 <sup>+0.7</sup> <sub>-0.4</sub>	208 <sup>+105</sup> <sub>-60</sub>	208 <sup>+105</sup> <sub>-80</sub>

<sup>a</sup> Number of disappearing C IV BAL troughs

<sup>b</sup> Fraction of disappearing C IV BAL troughs

<sup>c</sup> Number of quasars showing a disappearing C IV BAL trough

<sup>d</sup> Fraction of quasars showing a disappearing C IV BAL trough

<sup>e</sup> Number of quasars that transformed from BAL to non-BAL quasars

<sup>f</sup> Fraction of quasars that transformed from BAL to non-BAL quasars

<sup>g</sup> Average trough lifetime

<sup>h</sup> Lifetime of the BAL phenomenon along our line of sight